Available online at www.sciencedirect.com
SCIENCE DIRECT®
Journal of Chromatography A, 985 (2003) 519–529
JOURNAL OF CHROMATOGRAPHY A
www.elsevier.com/locate/chroma

Hyperlayer hollow-fiber flow field-flow fractionation of cells

Pierluigi Reschiglian[a,*], Andrea Zattoni[a], Barbara Roda[a], Leonardo Cinque[a], Dora Melucci[a], Byung Ryul Min[b], Myeong Hee Moon[c]

[a]*Department of Chemistry "G. Ciamician", Via Selmi 2, I-40126 Bologna, Italy*
[b]*Department of Chemical Engineering, Yonsei University, Seoul 120-749, South Korea*
[c]*Department of Chemistry, Pusan National University, Pusan 609-735, South Korea*

Abstract

Interest in low-cost, analytical-scale, highly efficient and sensitive separation methods for cells, among which bacteria, is increasing. Particle separation in hollow-fiber flow field-flow fractionation (HF FlFFF) has been recently improved by the optimization of the HF FlFFF channel design. The intrinsic simplicity and low cost of this HF FlFFF channel allows for its disposable usage, which is particularly appealing for analytical bio-applications. Here, for the first time, we present a feasibility study on high-performance, hyperlayer HF FlFFF of micrometer-sized bacteria (*Escherichia coli*) and of different types of cells (human red blood cells, wine-making yeast from *Saccharomyces cerevisiae*). Fractionation performance is shown to be at least comparable to that obtained with conventional, flat-channel hyperlayer FlFFF of cells, at superior size-based selectivity and reduced analysis time.

Keywords: Hollow fibers; Field-flow fractionation; Cells

1. Introduction

Field-flow fractionation (FFF) is a family of separation techniques able to fractionate, either on an analytical or on a micro-preparative scale for further characterization, a broad range of macromolecular, nano- and micrometer-sized particles [1]. Among the FFF techniques, flow FFF (FlFFF) shows the highest separation versatility. Classical FlFFF separators have a flat channel design, with the ribbon-like channel cut out from a thin plastic foil (spacer) with rectangular profile and tapered ends. FlFFF employs a secondary, transverse flow as external field. Other than a classical, flat-channel design, the idea of hollow-fiber (HF) membranes as cylindrical, micro-column channels for FlFFF was reported in 1974 [2]. Sample separation in HF FlFFF is structured by the force generated by the radial flow through the porous wall of the HF membrane. Since there is no influx from a secondary flow generator as in conventional, symmetrical FlFFF [3], the flow pattern in the HF FlFFF channel recalls the one in asymmetrical FlFFF (AsFlFFF) [4]. In HF FlFFF the flow that enters the HF channel inlet is divided into two parts: part of the flow penetrates the HF inner wall as radial flow and the rest exits from the HF channel outlet as axial flow. Sample components are separated because they are driven to different positions toward the inner wall of the HF membrane by the force exerted by the radial flow.

HF FlFFF ability to separate nano-sized particles was first described in few papers on separation of

*Corresponding author. Tel.: +39-51-209-9564; fax: +39-51-209-9456.
E-mail address: resky@ciam.unibo.it (P. Reschiglian).

0021-9673/02/$ – see front matter
PII: S0021-9673(02)01458-9

spherical polystyrene latex (PS) standards [5–10]. Further work was made at the separation of few proteins and water-soluble polymers [11,12] and synthetic organic-soluble polymers [13]. Significant improvements in particle separation by HF FlFFF have been shown in recent work, where efficiency normally achieved by conventional, flat FlFFF channels has been achieved through the optimization of the HF FlFFF channel and system design. Increase in separation speed and resolution has been first obtained for nano-sized particles [14] with further extension to a size as high as 1 μm [15].

In the case of submicrometer-sized particles, the sample components having small diameter have higher diffusion coefficients. By the action of the radial flow they reach an equilibrium distance from the fiber wall that is located further away than sample components of bigger size, and they are eluted first. Therefore, the elution order follows the increase in particle size, and it is referred to as normal mode [14]. Normal mode was the first elution mode studied in FFF, although ''anomalous'' retention of supramicrometer-sized particles was observed since early experimental FFF [16]. Large particles undergo, in fact, a negligible influence of diffusion in reaching their equilibrium positions across the channel. Larger particles protrude to faster streamlines of the parabolic flow profile than small particles do, and they are then swept down the channel earlier. The elution mode is, in fact, reversed with respect to the elution of submicrometer-sized particles. The definition of ''normal'' and ''reversed'' mode thus retains the definition logic of classical liquid chromatography, although it refers only to the elution order. In reversed mode, particles tend to migrate at an elevated position from the surface of the channel wall, at which they form a narrow layer (hyperlayer) because of the effect of hydrodynamic lift forces [17]. The elution mechanism is referred to as hyperlayer (hyp). The reversed mode with hyperlayer retention mechanism was applied in different FFF techniques to the fractionation of a wealth of particulate samples, at high size-based selectivity and short analysis time. Only very recently, however, a wider selection of membranes for HF FlFFF channels has been shown suitable for hyp HF FlFFF [18]. With respect to conventional, flat-channel FFF, the key advantage of the latest version of channels for hyp HF FlFFF lies in the instrumental simplicity and low cost. These features allow, in perspective, for disposable usage. Disposable HF FlFFF separators can be particularly appealing for analytical and micro-preparative sorting of cells, for which either sterility or the absence of sample carry-over are fundamental aspects. As a consequence, the extension of HF FlFFF to micrometer-sized analytes opens up new perspectives in the field of cell sorting.

Cell sorting is an outstanding topic in many fields, from diagnostics and biotechnology, to stem cell-assisted therapy and transplants. Since the early 1980s, the possibility to develop FFF-based cell sorting was established by Caldwell and co-workers in a pioneering work where they demonstrated the possibility to separate different types of cells of different characteristics [19]. More than a decade later, Chmelík and co-workers employed gravitational FFF (GrFFF) to sort mouse bone marrow stem cells that were re-transplanted after irradiation [20]. It was due to the extensive work of Cardot and co-workers [21] the development of biocompatible FFF instrumentation [22] for cell separation as well as the definition of sterilizable separators and appropriate methodological procedures to collect viable and reusable purified cells [23,24]. Bacterial cell sorting by separation methods is also of great interest since bacteria are used in diverse fields. Very recently, high-performance FFF-based cell sorting has been shown for mixtures of fimbriated/non-fimbriated *Escherichia coli* (*E. coli*) used for whole-cell vaccines [25]. The very first examples of HF FlFFF sorting of submicrometer-sized bacteria have been also recently reported. Different serotypes of deactivated *Vibrio cholerae* (*V. cholerae*) used for whole-cell vaccines have been efficiently fractionated and partly distinguished with performance comparable to that of classical FFF with flat channels [26].

In order to explore the possible use of hyp HF FlFFF for cell sorting, in this paper it is for the first time presented a feasibility approach to hyp HF FlFFF of micrometer-sized bacteria and of two different types of micrometer-sized cells. Well-characterized model samples are employed. Mixtures of fimbriated/non-fimbriated *E. coli* strains used for whole-cell vaccines are fractionated at performance comparable to that previously obtained with flat-

channel FFF [25]. High-performance separation of fresh human red blood cells (HRBCs) and wine-making yeast from *Saccharomyces cerevisiae* (*S. cerevisiae*) is also shown. Results were obtained with two different types of HF membranes: polysulfone (PSf) and chlorinated polyvinylchloride (cPVC). Mobile phase composition was studied in order to possibly reduce cell–HF membrane interactions. High sample recovery and negligible sample carry-over are found for HRBCs, as well as high sensitivity in monitoring osmolarity effects on their morphology. HRBCs and wine-making yeast are also sized by HF FlFFF calibration with PS. For HRBCs, results agree with size data obtained for HRBCs by uncorrelated, standard methods of clinical analysis. In the case of wine-making yeast, qualitative agreement is found with data obtained in previous work by uncorrelated sizing methods [27,28].

2. Basic theory

Particle retention in HF FlFFF follows the basic principle of FFF. Theory of HF FlFFF retention has been described in the literature [14,15,18]. For the reader's convenience, the fundamental expressions derived in the previous work on hyp HF FlFFF [18] are hereafter reported.

Retention ratio, that is $R = t_0/t_r$, can be expressed as:

$$R = 2\gamma \cdot \frac{d}{r_f} \tag{1}$$

where d is the particle diameter, r_f the inner fiber radius, and γ is the hydrodynamic correction factor, an empirical parameter that is related to particle morphology, field strength, and linear flow velocity of the mobile phase [18,29]. As with flat-channel hyp FlFFF, retention of supramicrometer-sized particles depends on hydrodynamic lift forces, which play an important role in lifting particles away from the HF inner wall. Lift forces effects are yet difficult to be fully described from first principles. As a consequence, particle retention in hyp HF FlFFF cannot be predicted from theory. A calibration procedure is commonly used to work out an empirical relationship between retention time (t_r) and particle diameter (d). This can be expressed with the following, well-known equation [29]:

$$\log t_r = \log t_{r1} - S_d \log d \tag{2}$$

where t_{r1} is the extrapolated retention time of a particle of unit diameter and S_d is the diameter-based selectivity, which is defined as

$$S_d = \left| \frac{\mathrm{d} \log t_r}{\mathrm{d} \log d} \right| \tag{3}$$

Since in hyp FlFFF retention is theoretically independent of particle density but shows dependent on shape, from linear regression on retention time data obtained for standard particles of known size (e.g., PS) it is possible to determine the size-based selectivity and, then, the particle diameter (or particle diameter distribution) of polydisperse, unknown particulate samples if the particle aspect ratio is not too high. By rearranging Eq. (2) one gets the expression to obtain the particle size of a given sample under conditions for which S_d is a constant:

$$d = \left(\frac{t_r}{t_{r1}} \right)^{-1/S_d} \tag{4}$$

In addition, the experimental parameters obtained from the calibration (S_d, t_{r1}) can be used to predict the particle diameter at which transition from normal to reversed elution mode occurs [18]:

$$d_i = \left(\frac{4kTt_{r1}}{3\pi\eta r_f U t_0 S_d} \right)^{1/(1+S_d)} \tag{5}$$

where k is the Boltzmann constant, T the temperature, U the radial flow velocity at the fiber wall, and η is the carrier viscosity. With supramicrometer-sized particles eluted in hyp HF FlFFF, S_d values have been always found higher than unity [18], as it is the case of conventional, flat-channel hyp FlFFF [30]. The corresponding values for d_i have been found in the range 0.3–0.8 μm, and dependent on flow-rate conditions [15,18].

3. Experimental

3.1. HF FlFFF channel

The HF channel was built up as previously

Table 1
Types of HFs

Type of HF material	M_r cutoff	HF inner radius (mm)	Manufacturer
Polysulfone (PSf)	30 000	0.410	SKU (South Korea)
Chlorinated PVC (cPVC)	50 000	0.440	Sambo (South Korea)

described [14,15,18,26]. HFs were made of PSf or cPVC. The fiber radius and the M_r cutoff values are listed in Table 1. Channel length was always 24 cm.

3.2. HF FlFFF configuration and operations

For this work, the HF FlFFF system configuration already reported in a previous work [26] was modified as shown in Fig. 1. The new scheme is proposed to allow for easier management of the complete run cycle. The cycle is constituted of three steps, each step corresponding to different flow-rates and flow patterns: (a) sample injection/focusing/relaxation, (b) channel elution, (c) system flow-feedback.

During steps b and c, one HPLC pump generates the required channel flow-rates, while for step a a second, syringe pump was also used. The HPLC pump was the Model 422 (Bio-Tek Kontron, Milan, Italy) and the syringe pump was the Model Pump11 (Harvard Bioscience, Holliston, MA, USA). Sample injection was made via a Model 7125 injection valve (Rheodyne, Cotati, CA, USA) equipped with an external 5.0-μl polyether ether ketone (PEEK) loop.

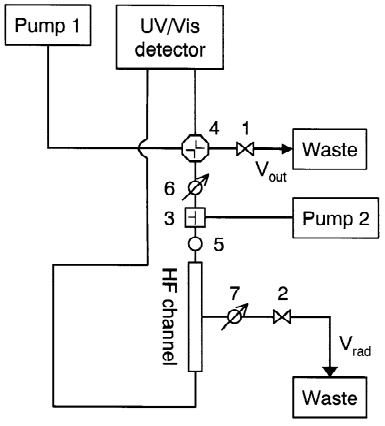

Fig. 1. Scheme of the HF FlFFF system. (1,2) Metering valves; (3) ''Tee'' valve; (4) four-way diagonal valve; (5) injector; (6,7) pressure gauges.

Flow conversions were made by using four- and three-way switching valves, as illustrated in Fig. 1. Flow rates at all waste outlets (V_{rad}, V_{out}, Fig. 1) were adjusted with the use of SS-SS2-VH Nupro metering valves (Nupro, Willoughby, OH, USA) (valves 1, 2, Fig. 1), and flow-rate values were measured by burettes and chronometer. Before sample injection, the injection/focusing/relaxation flow patterns (step a) were set via a three-way, tee valve (Hamilton, Reno, NV, USA) (valve 3, Fig. 1) and a four-way, diagonal flow valve (Upchurch, Oak Harbor, WA, USA) (valve 4, Fig. 1). The HPLC pump (pump 1, Fig. 1) and the syringe pump (pump 2, Fig. 1) were set at 0.180 and 0.050 ml min^{-1}, respectively. The sample focusing/relaxation process was then carried out for 3–5 min. The sample focusing position is dependent on the chosen ratio between the flow-rates generated by pumps 1 and 2, which, respectively, enter the HF channel from the outlet and the inlet. The focusing point was determined as previously described [18].

The elution flow pattern (step b) was set by turning off pump 2, and acting on valve 3 and valve 4, while pump 1 was set at a flow-rate (V_{in}) of 3.0 ml min^{-1}. These operations generate pressure pulses and variations of the mobile phase flow-rate that are responsible for the intense transient (void) peak observed at the beginning of the fractograms further reported in all figures. The required radial (V_{rad}) and axial (V_{out}) flow-rate values were pre-set by tuning valves 1 and 2. The flow-feedback step (step c) was set when the sample elution was finished. For system flow-feedback, the flow-rate from pump 1 was increased to a value of 6.0 ml min^{-1} and the flow pattern then reversed for at least 1 min from the detector outlet to the HF channel inlet, via valve 4. This caused the detector cell, the HF channel and the injection loop be back-flushed at high flow-rate and without field ($V_{rad}=0$) for system clean-up before the next run.

The model UV 6000 LP (ThermoQuest, Austin, TX, USA), high-sensitivity diode-array UV/Vis detector equipped with a fiber optic (FO) guide light-pipe cell was employed. Cell pathlength was measured with a spectroscopic standard, as described in previous work [26]. It resulted to be 4.55±0.32 cm.

3.3. Samples and mobile phases

For selectivity measurements, PS spherical standards from Duke Scientific (Palo Alto, CA, USA) were employed. Nominal diameters were 3.063±0.027, 4.000±0.033, 5.990±0.045 μm, hereafter referred to as PS 3, 4, 6.

Two different strains of deactivated *E. coli* from SBL Vaccin AB (Solna, Sweden) were analyzed: a fimbriated CS5 strain (batch No. 0398) and a non-fimbriated strain used for vaccine placebo (XC113 A2). Original samples were diluted in the mobile phase before the injection. *E. coli* were injected in a range of approximately 5000–20 000 cells.

Fresh human blood was drawn from donors under clinical control. Samples were collected in EDTA-containing tubes to inhibit coagulation. A 2-fold dilution was then performed in isotonic phosphate-buffered saline (PBS) (150 m*M*, i.e., 300 mOsm; pH 7.4) and samples were stored at 4 °C. They were analyzed within 4 days after further 1500–150-fold dilution in the chosen mobile phase. HRBCs were injected in a range of 7000–70 000 cells for each run. Certified determination of average HRBC concentration and average HRBC number distribution were obtained for all blood samples by standard methods of clinical analysis.

Commercial, dry wine-making yeast cells (*Saccharomyces cerevisiae*, strain INRA Narbonne 7013, from Gist-Brocades, Casteggio, Italy) were resuspended for 1 h in ultrapure water (Simplicity, Millipore, Bedford, MA, USA). Samples were stored at 4 °C and then diluted in the mobile phase before the injection of approximately 100 000 cells.

For PS, deactivated *E. coli* and yeast samples, the well-known solution for particle separation in FFF was used: FL-70 0.1% (v/v) (1.2 mOsm), NaN_3 0.002% (w/v) (0.62 mOsm). FL-70 is the trade name (from Fisher Scientific, Fair Lawn, NJ, USA) of a mixture of ionic/non-ionic surfactants made of 3.0% oleic acid, 3.0% Na_2CO_3, 1.8% Tergitol, 1.4% tetrasodium ethylenediamine tetraacetate, 1.3% triethanolamine, and 1.0% polyethylene glycol 400. Tris 0.125% (w/v) was added, if necessary. For fresh HRBCs the mobile phases were PBS solutions (pH 7.4) prepared at different osmolarity, added with 1 m*M* cholic acid.

4. Results and discussion

4.1. HF FlFFF of E. coli

In order to test separation performance, size-based selectivity was first measured in HF FlFFF with PSs of different size. The HF membrane was PSf. Regression analysis on Eq. (2) gives $\log t_r = (1.08\pm0.06)-(1.5\pm0.1)\log d$ ($r^2=0.94$, $n=12$) for $V_{out}=2.65$ ml min^{-1}, $V_{rad}=0.35$ ml min^{-1}, $V_{out}/V_{rad}=7.57$. The so-obtained size-based selectivity value ($S_d=1.5\pm0.1$) is very high and comparable to the values obtained in the previous work on hyp HF FlFFF of supramicrometer-sized PS, under similar flow-rate conditions and with the PSf HF channels [18]. Calculation of particle elevation at these flow-rate conditions has been also performed [18]. It has been therein shown that PS particles migrate at a distance from the channel wall which is much larger than the particle radius. This supports that the current HF FlFFF mechanism is hyperlayer.

Run-to-run reproducibility has been one of the major concerns in HF FlFFF, because of the possible membrane deformation during usage [14]. From previous work it is in fact known that PSf HFs are softer than cPVC and PAN HFs, and consequently they could be more easily deformed during usage, because of the backpressure generated by the HF FlFFF system. This deformation can be particularly severe at the relatively high flow-rate conditions used for hyp HF FlFFF. However, it has been also shown that when PSf HF channels were employed for HF FlFFF of *V. cholerae* [26], no significant membrane deformation occurred even after several runs, because of the very low backpressure generated by the used light-pipe detector cell. Such a detector cell has been then used in the present work as well. No significant variation of retention times was observed for HF FlFFF of PS with the HF PSf M_r 30 000 channels, under the same flow-rate conditions used

for the S_d determination. Channel life-times were not significantly different from those of HF channels in cPVC and PAN (ca. 30 runs). However, a systematic comparison between different types of HFs as it was performed in the first paper on hyp HF FlFFF is beyond the aims of this first application of hyp HF FlFFF to cells.

E. coli are rod-shaped cells, with fimbriated cells showing ''pili'' on the membrane [31]. Mixtures of the fimbriated and non-fimbriated strains here employed for HF FlFFF have been previously sorted by GrFFF and AsFlFFF [25]. In that work, a detailed description of the elution mechanism shows that these cells are eluted in the hyperlayer mode. For both fimbriated and non-fimbriated cells the average cell length has been, in fact, measured by scanning electron microscopy (SEM) on fractions collected after AsFlFFF. Cells resulted to be ca. 2 μm in length and 0.7 μm in width, which correspond to an aspect ratio of about 2.7. Separation between fimbriated and non-fimbriated *E. coli* has been thus shown to be due to differences in surface features rather than differences in size. Fig. 2 shows HF FlFFF of the fimbriated (CS5 0398 strain) and the non-fimbriated (XC113 A2) cells. Flow-rate conditions were $V_{out}=2.56$ ml min^{-1}, $V_{rad}=0.44$ ml min^{-1}, $V_{out}/V_{rad}=5.81$. A very large difference in retention between the strains can be observed, even higher than previously observed in AsFlFFF of fimbriated/non-fimbriated *E. coli* [25].

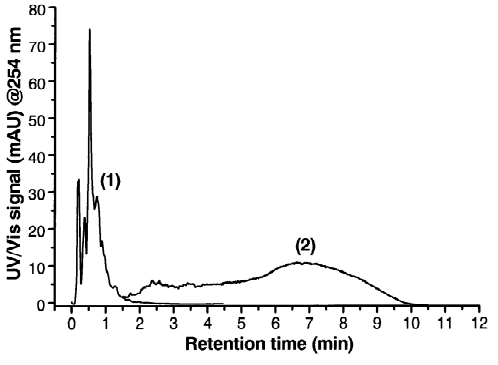

Fig. 2. HF FlFFF of *E. coli*. (1) Fimbriated strain C55 0398. (2) Non-fimbriated strain XC113 A2. Mobile phase: FL-70 0.1% (v/v), NaN_3 0.002% (w/v), Tris 0.125% (w/v). Flow rates: $V_{out}=2.56$ ml min^{-1}; $V_{rad}=0.44$ ml min^{-1}. PSf HF channel.

4.2. HF FlFFF of HRBCs

4.2.1. Retention

HRBCs are among the most characterized cells in biology. It is thus not surprising that HRBCs have been the workhorse for FFF of cells. Since more than a decade Cardot and co-workers have used HRBCs as model sample for FFF of cells [21]. Investigation on the influence of the ''multi-polydispersity matrix'' on retention, as well as on the optimization of the FFF systems and analysis procedures for fresh cells, was performed by means of extensive studies of HRBCs in GrFFF and sedimentation (Sd) FFF. In fact, very few examples of FlFFF of HRBCs have been up to now reported [32,33].

In Fig. 3 the dependence of HF FlFFF retention of HRBCs on the ratio between outlet flow-rate (V_{out}) and cross-flow-rate (V_{rad}) is shown. Because of the hyperlayer mechanism, retention depends on the balance between the force generated by the radial flow-rate and lift forces, which increase with increasing the channel flow-rate [18]. The retention behavior shown in Fig. 3 agrees with the hyperlayer mechanism. Retention levels decrease with increasing V_{out}/V_{rad}, because of the increasing contribution of lift forces. Moreover, the V_{out}/V_{rad} values correspond, in all cases, to conditions under which particles of same size as HRBCs migrate at a distance from the HF wall far larger than their size

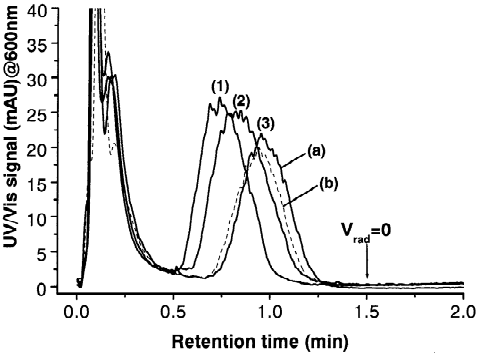

Fig. 3. HF FlFFF of HRBCs. Injected cells: 70 000. Effect of V_{out}/V_{rad} on retention: (1) $V_{out}=2.80$ ml min^{-1}, $V_{rad}=0.20$ ml min^{-1}; (2) $V_{out}=2.76$ ml min^{-1}, $V_{rad}=0.24$ ml min^{-1}; (3) $V_{out}=2.73$ ml min^{-1}, $V_{rad}=0.27$ ml min^{-1}. (a,b) Repeated runs. Mobile phase: isotonic PBS (300 mOsm), cholic acid 1 m*M*. cPVC HF channel.

[18]. It is finally noteworthy the generally short analysis time, which makes hyp HF FlFFF very competitive with respect to other FFF techniques used for HRBCs. The drastic reduction of the channel volume in HF FlFFF with respect to flat FFF channels shows, thus, the advances in performance/analysis time ratio which are typical of microcolumn separations. Reproducibility is also good, as shown by the repeated runs performed at the highest V_{rad} value (case 3, a and b). Good reproducibility and negligible sample carry-over have been already observed for HF FlFFF of deactivated *V. cholerae* [26].

4.2.2. Sample recovery and limit of detection

Sample recovery in HF FlFFF of HRBCs can test quantitative performance of HF FlFFF for cell sorting. For FFF of fresh cells, the dramatic effect of possible cell adhesion on the accumulation wall of the channel is, in fact, generally known. This can be particularly serious in HF FlFFF where the focusing/relaxation procedure is required before sample elution. Minimization of HRBC-channel adhesion was studied by Cardot and co-workers [34]. The use of plastic (hydrophobic) channel walls and the addition of bovine serum albumin (BSA) to the mobile phase were therein shown to increase cell recovery in SdFFF. However, in HF FlFFF the BSA could not be added to the mobile phase because it was retained under the flow-rate conditions used for HRBCs. Otherwise, the use of surfactants in the mobile phase can damage the HRBC membrane. In this work, for the first time the use of cholic acid in the mobile phase for FFF of HRBCs is shown. Bile acids (BAs) are amphipathic steroids from the catabolic pathway of cholesterol in the liver. Lipophilicity and detergent properties of BAs depend on the molecular structure [35]. Particularly, the critical micellar concentration (CMC) of the cholic acid (3α,7α,12α-trihydroxy-5β-cholan-24-oic acid) in PBS is in the range of 11–16 m*M* [35]. Such a relatively low CMC value indicates high detergent properties. Lipophilicity of cholic acid is also relatively high, even in the salified form at which it is present in PBS (pH 7.4) [36]. HRBC membrane has an asymmetric lipidic composition. The outer layer contains, above all, phosphatidylcholine, whereas phosphatidylethanolamine and phosphatidylserine are in the inner leaflet [37]. BAs dissolve in the membrane by intercalation of their molecules into the hydrophobic interior and they then influence both shape and resistance to hemolysis. It was determined that the solubilization degree of HRBC lipids in 1 m*M* BA solutions is as high as 3%, with corresponding percent of hemolysis [37]. For all the above reasons cholic acid was then used as surfactant and detergent modifier in the mobile phase for HF FlFFF of HRBCs at a concentration far below its CMC value. It is also known that BAs are generally adsorbed on apolar surfaces like the reversed-phases used in HPLC [38]. Lipophilicity of the cholic acid can thus be used also to polarize the relatively hydrophobic surface of the HF channel and to reduce adhesion between HRBCs and the inner surface of the HF channel. BAs can also complex calcium and magnesium in aqueous solutions [39]. Their use is therefore interesting to also inhibit blood cell coagulation.

Absolute recovery in HF FlFFF can be evaluated by the ratio between the band area values obtained for in-channel and off-channel sample injections. If band areas are the same, the absolute recovery is, of course, total (100%). The presence of linear recovery can be ascertained by the evaluation of fractogram area values obtained for the injection of different sample masses. It is noteworthy to recall that a high, absolute recovery allows for micro-preparative scale applications, while non-linear recovery may suggest sample carry-over, a drawback in the separation of biosamples. In Fig. 4 are reported the HF FlFFF fractograms obtained for different numbers of injected HRBCs. The HRBC concentration in the fresh blood sample was measured to be 4.34×10^{9} HRBCs ml^{-1}. Fractogram a corresponds to an injection of 70 000 HRBCs that gave an area of 5.77×10^{-3} min, while the injection of 7000 HRBCs gave an area of 0.669×10^{-3} min (fractogram b). In order to determine the absolute recovery, the same number of HRBCs injected to obtain the fractogram a was also injected off-channel. The so-obtained peak gave an area of $(8.5\pm0.2)\times10^{-3}$ min. The absolute recovery results to be relatively high: 78% of the 7000 injected HRBCs. From the ratio between the area values of the a/b fractograms in Fig. 4, non-linear recovery is, however, observed: (a) 68% recovery of 70 000 HRBCs; (b) 78% recovery of 7000 HRBCs.

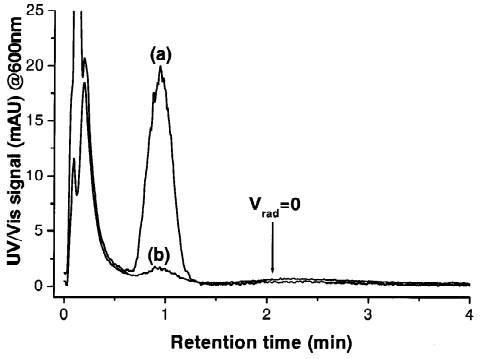

Fig. 4. Quantitative analysis in HF FlFFF of HRBCs. Injected cells: (a) 70 000; (b) 7000. Mobile phase: isotonic PBS (300 mOsm), cholic acid 1 m*M*. $V_{out}=2.73$ ml min^{-1}, $V_{rad}=0.27$ ml min^{-1}. cPVC HF channel.

Otherwise, this finding may indicate that the lower the number of injected cells, the higher the absolute recovery. In fact, the injection of 7000 HRBCs (Fig. 4, fractogram b) gives a signal intensity that is comparable to the signal intensities typically obtained in FFF for the injection of a comparable number of HRBCs [22,23], and that appears to be above the limit of detection. This finding suggests that increase in sample recovery may be obtained by the injection of an even lower number of cells. The limit of detection was determined with supramicrometer-sized PS standards, since it is known that in this size range the optical extinction properties of particles are relatively independent of their chemical composition [40]. Different and known masses of PS 4 were run under the same flow conditions used for HRBCs, and peak areas were measured. Regression analysis gave: area [mAU min]$=(7.6\pm0.1)\times10^{-3}$ mass [ng]$+(0.6\pm0.2)$ ($n=7$). This gives a limit of detection for PS 4 of 120 ng, which corresponds to 3500 particles. A systematic study on sample recovery and limit of detection values in HF FlFFF of cells is beyond the aims of the present paper. Optimization of the mobile phase composition with the choice of the most suitable BA modifier and relevant concentration is in progress. All the work was performed with the cPVC of HF membranes. In order to optimize HF FlFFF for HRBCs further work is also needed to compare different types of HFs. In all the HRBC fractograms, a low-amplitude band after the main band was also observed when the field was stopped, as shown in Fig. 4. This indicates that some reversible cell–channel adhesion during the analysis contributed to recovery losses. Otherwise, the possible onset of irreversible cell–channel adhesion is known to be very critical in cell sorting by FFF. However, the values of absolute recovery here found can be satisfactory in all cases if the possible disposable usage of the channel is considered.

4.2.3. Morphological analysis

Morphology indexes of HRBCs are known to depend on medium osmolarity [41]. The osmolarity effects on HRBCs elution in SdFFF were studied by Cardot and co-workers [42]. Fig. 5a reports the effect of a reduction in the mobile phase osmolarity on HF FlFFF retention of HRBCs. As expected, with respect to the elution in isotonic PBS (case 2), reduction and increase in retention are observed, respectively, in hypotonic (case 1) and hypertonic PBS (case 3). It is moreover known that the HRBC sphericity index can be defined as:

$$I=\frac{4.84V^{2/3}}{S} \quad (6)$$

where S is the mean surface of the HRBC membrane and V the mean HRBC volume. It changes from 0.7 in isoosmolar (300 mOsm) solution (i.e., PBS 150 m*M*) to 1.0 in 170 mOsm solution (i.e., PBS 85 m*M*) [41]. When $I=1.0$ the HRBC is perfectly spherical and, therefore, its hydrodynamic diameter corresponds to $1.24V^{1/3}$. The average HRBC volume in isotonic medium was given, for the supplied fresh blood sample here employed, by means of standard methods of clinical analysis (i.e., Coulter counter). It resulted to be $V=90.4$ μm^3 which, from Eq. (6), corresponds to an average HRBC surface of $S=139$ μm^2. This latter value is in excellent agreement with data reported in the literature, which gives $S=140$ μm^2 [41]. With the mobile phase osmolarity for which $I=1.0$ (PBS 85 m*M*), the value of S is known to be equal to the HRBC surface in isotonic conditions [41]. The average diameter for spherical HRBCs can be thus calculated as 6.6 μm. With respect to GrFFF and SdFFF, in hyp HF FlFFF retention depends on the hydrodynamic diameter and shape of particles but it is independent of particle density. As a consequence, if the effects of different

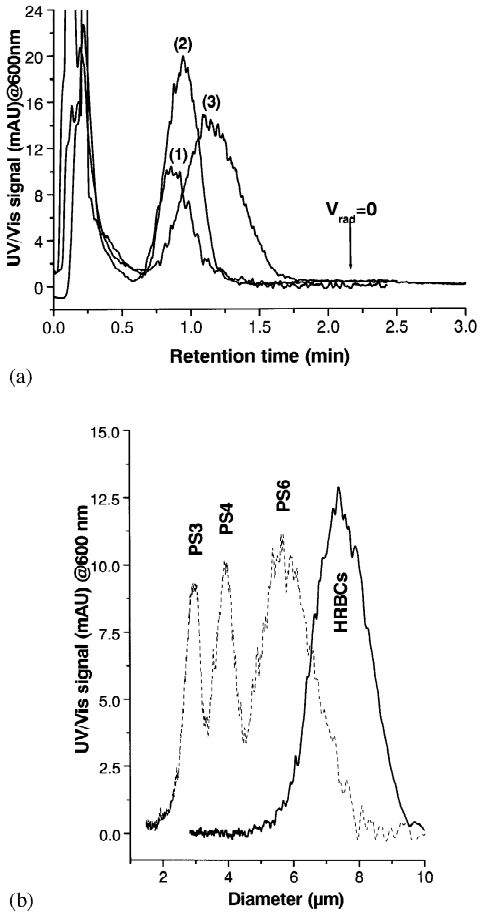

Fig. 5. Morphology-based sorting of HRBCs by HF FlFFF. cPVC HF channel. Injected cells: 70 000. (a) Mobile phase: PBS, cholic acid 1 m*M*; (1) hypotonic (225 mOsm); (2) isotonic (300 mOsm); (3) hypertonic (450 mOsm). (b) Mobile phase: PBS 85 m*M*, cholic acid 1 m*M*. $V_{out}=2.73$ ml min^{-1}, $V_{rad}=0.27$ ml min^{-1}. Comparison with PS (dashed line); conversion from t_r to diameter scale by Eqs. (2) and (3).

particle flexibility are not taken into account, in 170 mOsm the spherical HRBCs ($I=1.0$) should be eluted at the same retention time as PS of same size. Fig. 5b reports the HF FlFFF fractogram of HRBCs in PBS 85 m*M* (170 mOsm) compared to the fractogram of a mixture of PS standards of known diameter, which was obtained under the same flow-rate conditions used for HRBCs. From the PS mixture fractogram, regression analysis gives $\log t_r = (1.09\pm0.01)-(1.37\pm0.02)\log d$ ($r^2=0.999$, $n=9$), from which the size-based selectivity S_d results to be 1.37. From this size-based selectivity value one can then convert the retention time axis to the diameter axis to calculate the average hydrodynamic radius of spherical HRBCs from retention time of the peak barycenter. This results to be 7.22 ± 0.06 μm, which agrees with the diameter value above calculated from the average HRBC surface when HRBCs become spherical (170 mOsm, that is PBS 85 m*M*). In fact, it should be considered that the standard method of clinical analysis employed for the evaluation of the average HRBC volume (i.e., Coulter counter) gives a number-average value, whilst the value obtained from conversion of the HF FlFFF band barycenter is a cross-section distribution average [40]. Its conversion to a number-average value would, indeed, give a lower value, in closer agreement with the number-average value determined by Coulter counter. This conversion, however, requires the application of turbidimetric methods in flow-assisted separation techniques [40], which is beyond the aim of the present paper. Possible differences in HRBC flexibility with respect to PS and the possible errors in retention time measurements at such short analysis times must be also taken into account. Results obtained from Fig. 5a,b demonstrate the interesting capabilities of hyp HF FlFFF for morphological sorting of fresh cells like HRBCs.

4.3. HF FlFFF of yeast

Active dry wine yeast is currently employed as a starter for commercial wine production. SdFFF showed suitable to monitor the growth of yeast cells by fractionation after cultivation [43]. Sanz and co-workers have recently employed GrFFF to fractionate and distinguish different types of commercial, dry wine-making yeast from *S. cerevisiae* [27,28].

Fig. 6 reports HF FlFFF of a commercial strain of dry wine-making yeast from *S. cerevisiae*. The HF membrane used was PSf of M_r 30 000. The fractogram of a mixture of PS obtained at the same flow-rate conditions used for the yeast sample is superimposed in Fig. 6. These flow-rate conditions were those employed for the regression analysis with PS discussed in Section 4.1, from which $S_d=1.5\pm0.1$ was obtained. From this S_d value one gets (Eq. (4)) the hydrodynamic diameter of the yeast cells as 4.8 ± 0.3 μm. Although yeast cells cannot be consid-

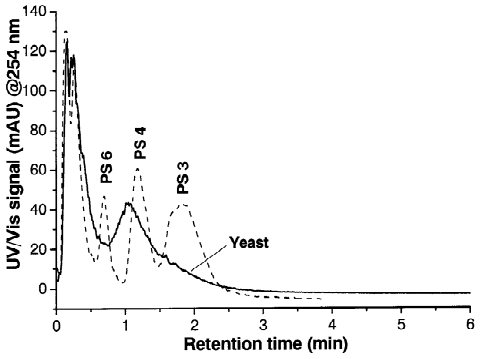

Fig. 6. HF FlFFF of wine-making yeast. Injected cells: $\approx 10^5$. Comparison with PS (dashed line). Mobile phase: FL-70 0.1% (v/v), NaN_3 0.002% (w/v), Tris 0.125% (w/v). Flow rates: $V_{out} = 3.0$ ml min^{-1}, $V_{rad} = 0.34$ ml min^{-1}. PSf HF channel.

ered as perfectly spherical, this value is comparable to the cell size of other types of wine-making yeast from *S. cerevisiae*, which has been determined by the Coulter counter measurements performed in previous GrFFF of wine-making yeast [27,28]. It is noteworthy that HF FlFFF shows here, with quite shorter analysis time, a fractionation performance that is, at least, comparable to that obtained in SdFFF or GrFFF of yeast cells.

5. Conclusions

Different types of cells have been fractionated with performance at least comparable to that of conventional, flat-channel FFF methods. The intrinsic features of the HF FlFFF channels here employed indicate, for hyp HF FlFFF, interesting perspectives for cell sorting, firstly because of the low cost and short analysis time. Secondly, with respect to SdFFF and GrFFF that have been up to now the most employed FFF techniques for cell sorting, HF FlFFF can avoid sample carry-over and sterility issues, because of the potentially disposable use of the channels.

In order to extensively apply hyp HF FlFFF to living cell sorting, cell viability after fractionation must be accurately tested. However, it was shown that FFF is a ''soft'' separation method for sorting living cells, the viability of which was generally shown not to be affected by elution. Sample recovery optimization in hyp HF FlFFF is also required for high throughput of sorted cells. Towards this end, the use of BAs as surfactant and detergent modifiers in the mobile phase has shown interesting features in the case of HRBCs. Work is in progress to test BA-modified, optimized mobile phases for HF FlFFF of HRBCs and of other cells.

HF FlFFF can be also used to isolate and recognize few bacteria and other cells in complex samples. In this case, however, highly specific and ultrasensitive detection methods must be coupled with HF FlFFF.

Acknowledgements

Hollow fibers were kindly supplied by SKU and Sambo (South Korea). *E.coli* strains were supplied by SBL Vaccin AB (Solna, Sweden), within Leonardo-EXCHANGE 2001, financial program for researchers mobility from the University of Bologna to small and medium enterprises within the EU. LC's research stay at the Department of Chemical Engineering, Yonsey University, Seoul (South Korea), was kindly supported by the Faculty of Science of the University of Bologna and by Yonsei University. Fresh blood samples were supplied and clinically tested by the Department of Internal Medicine and Gastroenterology, University of Bologna. E. Whitmore-Carlsson, SBL Vaccin, is duly acknowledged for accurate details on sample specifications and the helpful discussion. Thanks also goes to M. Massari for the experimental work performed, and to A. Roda for the helpful discussion on the properties of bile acids.

References

[1] J.C. Giddings, Science 260 (1993) 1456.
[2] H.-L. Lee, J.F.G. Reis, J. Dohner, E.N. Lightfoot, AIChE J. 20 (1974) 776.
[3] S.K. Ratanathanawongs-Williams, in: M.E. Schimpf, K. Caldwell, J.C. Giddings (Eds.), Field-Flow Fractionation Handbook, Wiley-Interscience, New York, 2000, Chapter 17.
[4] K.-G. Wahlund, in: M.E. Schimpf, K. Caldwell, J.C. Giddings (Eds.), Field-Flow Fractionation Handbook, Wiley-Interscience, New York, 2000, Chapter 18.
[5] A. Carlshaf, J.A. Jönsson, J. Chromatogr. 461 (1988) 89.

[6] J.A. Jönsson, A. Carlshaf, Anal. Chem. 61 (1989) 11.
[7] J.A. Jönsson, A. Carlshaf, J. Microcol. Sep. 3 (1991) 411.
[8] J. Granger, J. Dodds, Sep. Sci. Technol. 27 (1992) 1691.
[9] A. Carlshaf, J.A. Jönsson, Sep. Sci. Technol. 28 (1993) 1031.
[10] A. Carlshaf, J.A. Jönsson, Sep. Sci. Technol. 28 (1993) 1191.
[11] J.E.G.J. Wijnhoven, J.-P. Koorn, H. Poppe, W.Th. Kok, J. Chromatogr. A 699 (1995) 119.
[12] J.E.G.J. Wijnhoven, J.-P. Koorn, H. Poppe, W.Th. Kok, J. Chromatogr. A 732 (1996) 307.
[13] M. van Bruijnsvoort, W.Th. Kok, R. Tijssen, Anal. Chem. 73 (2001) 4736.
[14] W.J. Lee, B.-R. Min, M.H. Moon, Anal. Chem. 71 (1999) 3446.
[15] M.H. Moon, K.H. Lee, B.-R. Min, J. Microcol. Sep. 11 (1999) 676.
[16] K. Caldwell, T.T. Nguyen, M.N. Myers, J.C. Giddings, Sep. Sci. Technol. 14 (1979) 335.
[17] K. Caldwell, in: M.E. Schimpf, K. Caldwell, J.C. Giddings (Eds.), Field-Flow Fractionation Handbook, Wiley-Interscience, New York, 2000, p. 79, Chapter 5.
[18] B.-R. Min, S.J. Kim, K.-H. Ahn, M.H. Moon, J. Chromatogr. A 950 (2002) 175.
[19] K. Caldwell, Z.-Q. Cheng, P. Hradecky, J.C. Giddings, Cell Biophys. 6 (1984) 233.
[20] E. Urbankova, A. Vacek, J. Chmelík, J. Chromatogr. B 687 (1996) 449.
[21] A. Lucas, F. Lepage, Ph.J.P. Cardot, in: M.E. Schimpf, K. Caldwell, J.C. Giddings (Eds.), Field-Flow Fractionation Handbook, Wiley-Interscience, New York, 2000, Chapter 29.
[22] J.M. Metreau, S. Gallet, Ph.J.P. Cardot, V. LeMaire, F. Dumas, A. Hernvann, S. Loric, Anal. Biochem. 251 (1997) 178.
[23] S. Rasouli, E. Assidjo, Ph.J.P. Cardot, J. Chromatogr. B 754 (2001) 11.
[24] S. Battu, A. Roux, S. Delebasee, C. Bosgiraud, Ph.J.P. Cardot, J. Chromatogr. B 751 (2001) 131.
[25] P. Reschiglian, A. Zattoni, B. Roda, S. Casolari, M.H. Moon, J. Lee, J. Jung, K. Rodmalm, G. Cenacchi, Anal. Chem. 74 (2002) 4895.
[26] P. Reschiglian, B. Roda, A. Zattoni, B.-R. Min, M.H. Moon, J. Sep. Sci. 25 (2002) 490.
[27] R. Sanz, L. Puignou, P. Reschiglian, M.T. Galceran, J. Chromatogr. A 919 (2001) 339.
[28] R. Sanz, B. Torsello, P. Reschiglian, L. Puignou, M.T. Galceran, J. Chromatogr. A 966 (2002) 135.
[29] S. Lee, J.C. Giddings, Anal. Chem. 60 (1988) 2328.
[30] P. Reschiglian, D. Melucci, A. Zattoni, L. Malló, M. Hansen, A. Kummerow, M. Miller, Anal. Chem. 72 (2000) 5945.
[31] J.P. Nataro, J.B. Kaper, Clin. Microbiol. Rev. 11 (1998) 142.
[32] B.N. Barman, E.R. Ashwood, J.C. Giddings, Anal. Biochem. 212 (1993) 35.
[33] B.N. Barman, J. Colloid Interface Sci. 167 (1994) 467.
[34] T. Chianéa, Ph.J.P. Cardot, E. Assidjo, J. Monteil, P. Krausz, J. Chromatogr. B. 734 (1999) 91.
[35] A. Roda, H.F. Hofmann, K.J. Mysels, J. Biol. Chem. 258 (1993) 6361.
[36] M. Vadner, S. Lindenbaum, J. Pharm. Sci. 71 (8) (1992) 881.
[37] G. Salvioli, A. Mambrini, R. Lugli, R. Bertolani, E. Zirilli, in: L. Barbara, H. Dowling, A.F. Hofmann, E. Roda (Eds.), Recent Advances in Bile Acids Research, Raven Press, New York, 1985, pp. 17–23.
[38] R. Kaliszan, J. Chromatogr. 270 (1981) 71.
[39] A.F. Hofmann, in: J.G. Forte (Ed.), Handbook of Physiology. The Gastrointestinal System. Salivary, Pancreatic, Gastric and Hepatobiliary Secretion, Section 6, Volume 3, American Physiological Society, Bethesda, 1989, Chapter 28.
[40] P. Reschiglian, A. Zattoni, D. Melucci, G. Torsi, Rev. Anal. Chem. 20 (2001) 239.
[41] R.S. Weinstein, in: D.N. Surgenor (Ed.), 2nd edition, The Red Blood Cell, Vol. 1, Academic Press, New York, 1974.
[42] N.E. Assidjo, T. Chianéa, I. Clarot, M.F. Dreyfuss, Ph.J.P. Cardot, J. Chromatogr. Sci. 37 (1999) 229.
[43] S. Hofstetter-Kuhn, T. Rosler, M. Ehrat, H.M. Widmer, Anal. Biochem. 206 (1992) 300.